

COVER PAGE

Document downloaded by @DAEL

Fri Nov 20 03:57:18 2026
For personal use

When automatic English translation is provided, only the original document is authentic.
The EAA cannot be held responsible of any translation error

Bibliographical reference

Efficient Modelling of Absorbing Boundaries in Room Acoustic FE Simulations, Marc Aretz and Michael Vorländer, Acta Acustica **vol. 96** (Number 6), 2010, pp. 1042-1050

DOI
https://doi.org/10.3813/AAA.918366

ACTA ACUSTICA UNITED WITH ACUSTICA
Vol. 96 (2010) 1042 – 1050

DOI 10.3813/AAA.918366

Efficient Modelling of Absorbing Boundaries in Room Acoustic FE Simulations

Marc Aretz, Michael Vorländer
Institute of Technical Acoustics, RWTH Aachen University, 52066 Aachen, Germany.
[mar, mvo]@akustik.rwth-aachen.de

Summary
Thanks to the rapidly increasing computational power of contemporary computer systems, acoustic finite element (FE) applications are nowadays widely used to predict the modal behaviour of airborne and structure-borne sound waves in enclosed cavities. In room acoustics it is by now mostly possible to simulate the whole frequency range below the Schroeder frequency using FEM in reasonable simulation times, thus making it a promising contender for extending the validity of typically ray-based room acoustic simulations to lower frequencies. However, while contemporary CAD and meshing tools facilitate the design of high quality geometric models with regular and sufficiently fine meshes, the Achilles' heel of room acoustic FEM simulations appears to be the realistic representation of the room boundaries.
The present study investigates the influence of different boundary representations of porous absorbers on the simulated sound field in small rooms. Therefore measurements and FE simulations of the sound field in a scale model room with a well defined geometry and variable boundary conditions are conducted. Two different approaches are followed to model the porous absorbers on the room boundaries. Firstly the absorber layers are modelled with their exact 3D dimensions using an 'equivalent homogeneous fluid' (EHF) model. Secondly the acoustic characteristics of a porous absorber are modelled by an acoustic surface impedance for either normal or field/diffuse incidence, which is determined by measurement or model calculation. The paper clearly points out the limitations of the applied boundary models and also brings out the differences between these models. As a conclusion the paper shows that by using field incidence impedances instead of normal incidence impedances the quality of room acoustic FE simulation results can in some cases be increased considerably and comparable results to those obtained with a 3D absorber model can be achieved even for non-locally reacting materials.

PACS no. 43.55.Ev, 43.55.Ka, 43.58.Bh

1. Introduction

The airborne sound field in an enclosed cavity can be fully described as a function of its room geometry, source characteristics and the acoustic characteristics of its boundaries. In the field of room acoustic simulation techniques it is mostly the latter which causes acoustic practitioners and academics trouble. Three major questions arise in this context: First, what is the best way to model the characteristics of acoustic room boundaries? Second, how can the required input data for the acoustic boundary model be measured most reliably? And third, which amount of simplification in the boundary model and uncertainty in the measured input data is acceptable, so that no detrimental effects are caused to the subjective perception of the simulated sound field in the room?

While in the field of geometrical acoustics (GA) these questions have received considerable attention and there exist large material parameter databases [1] for typically used materials in room acoustics, only little is found with regard to room acoustic FE simulations. Moreover, since the boundary models and the required input data for FE and GA simulations differ considerably, the material parameter databases and uncertainty guidelines used for the latter can not easily be used or extended to the FE domain.

In contrast to energy-based GA simulations, where the room boundaries are generally characterized by their acoustic absorption and scattering coefficients, wave-based simulation methods such as the FEM necessitate the specification of the acoustic surface impedance or even coupling conditions of the fluid domain to a structure and/or porous absorber domain, to model the interaction of the sound field with the acoustic boundary. The focus of this paper concerns the efficient modelling of porous boundaries in room acoustic FE simulations. We therefore compare measured room transfer functions (RTF) obtained in a damped scale model room, to simulated RTFs, which were obtained by either using impedance boundary conditions for normal and field incidence or a coupled 3D FE absorber model. Taking into account that using a

Received 19 November 2009,
accepted 8 July 2010.

© S. Hirzel Verlag · EAA

Document downloaded by @DAEL, 2026-11-20 03:57:21 - personal use only

coupled 3D absorber model is much more costly in terms of computation time and model complexity compared to an impedance boundary condition, it is worthwhile investigating in which cases an actual benefit can be expected from using such complex models.

The subsequent section shortly summarizes the basics of FEM in a fluid domain. Then the boundary models are presented and their differences and limitations are pointed out. section 4 compares the measured and simulated RTFs obtained with the different boundary models.

2. Finite element fluid model

The wave propagation in a fluid medium in an enclosed cavity Ω can generally be described by the Helmholtz equation with given admittance (Robin) boundary conditions on the boundaries Σ_A and velocity (Neumann) conditions on the boundaries Σ_v of the fluid domain. The governing equations of the fluid FEM are derived by writing the Helmholtz equation and the boundary conditions in an integral form and multiplying by an arbitrary weighting function $\bar{w}$,

$$\int_\Omega \bar{w}\left(\Delta p + k^2 p\right) \mathrm{d}\Omega + \int_{\Sigma_v} \bar{w}\left(-\frac{\partial p}{\partial \boldsymbol{n}} - \mathrm{j}\omega\rho_F v_n\right) + \int_{\Sigma_A} \bar{w}\left(-\frac{\partial p}{\partial \boldsymbol{n}} - \mathrm{j}\omega\rho_F A_n p\right) = 0, \tag{1}$$

where p is the sound pressure, ω the harmonic frequency, j the complex number, k the propagation constant and ρ_F the fluid density. A_n gives the admittance for normal incidence and v_n the normal velocity at the corresponding fluid boundaries Σ_A and Σ_v respectively. By discretization of the spatial domain into finite elements, which is often referred to as "meshing", and limitation of the solution space of the pressure and weighting functions in each element to a polynomial approximation, the following system of FE equations can be derived for the fluid domain,

$$\left(\boldsymbol{K}_F + \mathrm{j}\omega\boldsymbol{A}_F - \omega^2\boldsymbol{M}_F\right)\boldsymbol{p} = \mathrm{j}\omega\boldsymbol{f}_v, \tag{2}$$

where the matrices $\boldsymbol{K}_F$ and $\boldsymbol{M}_F$ are called compressibility and mass matrix respectively, the matrix $\boldsymbol{A}_F$ comprises the boundary terms for the surfaces with given admittance conditions and the right-hand side vector f_v comprises the excitation of the sound field by the surfaces with given velocity conditions. The pressure field in the fluid domain can then be calculated by inversion of the given system of equations. A detailed introduction to the FEM in fluid acoustics is given in [2].

It can be shown that for increasing fineness of the discretization or alternatively an increasing order of the polynomial approximation, the FE solution converges to the true (analytic) solution for a given fluid domain and boundary conditions. However, in typical situations where we want to simulate the sound field in an already existing or planned room, we frequently face the problem that we have to identify realistic models for the boundaries of the fluid domain and that appropriate input parameters of these models have to be determined by measurement. The subsequent section therefore introduces two different approaches for the consideration of porous absorbers in room acoustic FE simulations and discusses the influence that these boundary representations exert on the sound field in the fluid domain.

3. Porous absorber models in room acoustic FEM

In room acoustic FE applications porous absorbers can either be modelled by an appropriate impedance boundary condition or by a full 3D-FE absorber model, which is coupled to the FE fluid domain. Acoustic surface impedances of porous absorbers can either be determined by measurement or by calculation based on a physical model of the wave propagation inside the absorber. These physical models can be roughly divided into models considering a rigid or an elastic absorber skeleton. A well-established model for porous absorbers with a rigid skeleton is the so-called 'equivalent homogeneous fluid' (EHF) approach, which owes much of its derivation to the theory of lossy electric transmission lines. This theory models a porous absorber as a damped fluid medium, where the complex propagation constant Γ_a and the characteristic impedance Z_a are derived as a function of either physically, phenomenologically or empirically based absorber parameters.

The original theory and the corresponding relations for Γ_a and Z_a were introduced by Zwikker and Kosten [3] in 1949, who based their derivation on heuristic differential equations to model the wave propagation in a porous absorber based on phenomenological absorber parameters. Other rigid skeleton approaches based for example on the models by Rayleigh [4, Vol. II, pp. 319-333] or again Zwikker and Kosten [3] have studied the wave propagation inside a porous absorber on a more microscopic scale, by analyzing the wave motion in a pore of a certain shape considering viscous and thermal effects. Although these approaches present a more rigorous approach to the physical effects inside a porous absorbers they inevitably neglect aspects regarding the complex shape and arrangement of pores in typically used fibrous absorbers. More recent semi-phenomenological models have extended these microscopic models to more general micro-geometries. A review of these semi-phenomenological models can for example be found in [5, pp. 73ff]. However, these models necessitate a hard experimental characterization of the porous absorber material. In order to simplify the experimental characterization of a porous absorber, various empirically based relations for Γ_a and Z_a have emerged, like the Delany-Bazley [6] or the Komatsu [7] models. These models use a large set of measured data to establish empirical relations for Γ_a and Z_a as a function of the flow resistivity of an absorber (as well as frequency, density of air and the sound speed in air).

Although there exist much more complex absorber models like the Biot model [8], which also accounts for

Document downloaded by @DAEL, 2026-11-20 03:57:21 - personal use only

the motion of the absorber skeleton and thus is based on a coupled formulation for the wave propagation of fluid and structural waves in the absorber, the EHF model is often considered adequate to realistically model the energy dissipation in typically used porous absorbers (fibrous or foam absorbers with high porosity). This has different reasons. According to Mechel [9, pp. 75ff] (a) the structural waves in typical porous absorbers are generally highly damped due to friction between the fibres and thus only have small amplitudes, (b) the thickness of room acoustic absorbers is often small compared to the structural wave lengths at low frequencies and (c) at high porosities ($> 90\%$) the structural frame has generally a negligible effect on the interaction of a porous absorber with an external fluid sound field, at least if the absorber is not covered with an adhesive airtight foil. Moreover, the high complexity of the Biot Model results in an increased number of difficult-to-measure model parameters, which necessitates time-consuming and complex measurement setups for the determination of these parameters. These model parameters include the tortuosity of the material, the elastic constants of the absorber skeleton and a factor relating to the pore shape[1]. A complete revision of the different empirical and phenomenological models introduced in this section can be found in [9] and [5].

In the course of this study we use the original Zwickker/Kosten model and recent empirical relations by Komatsu to calculate the acoustic surface impedances for normal and field incidence on a rigidly backed single layer porous absorber. As a reference we also use measured acoustic impedances for normal incidence which are obtained in a Kundt's tube[2]. In addition to the impedance boundary representation, we have implemented a 3D absorber model in our FE simulation software, which is also based on the original model by Zwikker and Kosten. We can thus compare the influence of different models of the same porous absorber on the RTF in a room acoustic FE simulation and also compare these results to measurements conducted in a real room.

3.1. Propagation constant and characteristic impedance in the EHF model

Zwikker/Kosten model [3]

Since the EHF model neglects the microscopic fine structure of the porous absorber and assumes a fixed structural frame, the only degree of freedom is the mean pressure in the absorber pores. Assuming further that the wave propagation is caused by an interchange between spatially distributed potential and kinetic energy storages in the absorber, Zwikker and Kosten derive the complex propagation constant Γ_a and the characteristic impedance Z_a as follows:

$$\Gamma_a = \mathrm{j}k_0\sqrt{\chi\kappa_{eff}\left(1-\mathrm{j}\frac{\sigma_v\Xi}{\chi\omega\rho_0}\right)}, \tag{3}$$

$$Z_a = \frac{Z_0}{\sigma_v}\sqrt{\frac{\chi}{\kappa_{eff}}\left(1-\mathrm{j}\frac{\sigma_v\Xi}{\chi\omega\rho_0}\right)}, \tag{4}$$

where Ξ is the static flow resistivity, σ_v the volume porosity, χ the structure factor and κ_{eff} the adiabatic exponent of air, which is corrected for effects due to thermal relaxation in the absorber. For a given absorber, the static flow resistivity and volume porosity are generally determined by straightforward measurement techniques. However, the structure factor, which is often considered as a tweaking factor for all the effects that are neglected in the model (typically values range from 1.0 to 1.3), and the corrected adiabatic coefficient (frequency dependant between 1.41 for low and 1.0 for high frequencies) are usually estimated or simply set equal to 1 (cf. [9, pp. 97]).

Komatsu model [7]

In contrast to the Zwikker/Kosten model, the Komatsu model is an empirically based two parameter model for fibrous sound-absorbing materials, which specifies Γ_a and Z_a as a function of the flow resistivity Ξ and frequency f:

$$\Gamma_a = \frac{2\pi f}{c_0}\left[0.0069\left(2-\lg\frac{f}{\Xi}\right)^{4.1} + \mathrm{j}\left(1+0.0004\left(2-\lg\frac{f}{\Xi}\right)^{6.2}\right)\right], \tag{5}$$

$$Z_a = \rho_0 c_0\left[1+0.00027\left(2-\lg\frac{f}{\Xi}\right)^{6.2} - \mathrm{j}0.0047\left(2-\lg\frac{f}{\Xi}\right)^{4.1}\right]. \tag{6}$$

It has already been mentioned that there exist various more of these empirical relations for porous absorbers, which all yield similar but slightly different absorption characteristics for a given porous absorber. However, for the sake of clarity we will only include the Komatsu model in this study in order to illustrate the differences between a model based on physically motivated differential equations and an empirical curve fitting model.

3.2. Impedances for normal and field incidence using a 1D transmission line model

The acoustic impedance $Z(f,\Theta_i)$ at a boundary surface is defined as the ratio of sound pressure p and surface normal velocity v_n which are obtained when a plane wave is incident at an angle Θ_i to the surface normal. Under the assumption that a porous absorber can be described by an EHF model, the impedance of a rigidly backed single layer

[1] Detailed information on measurement techniques for the determination of these parameters and further references on this topic can be found in [9, pp. 519ff]

[2] All measurements have been carried out following the transfer function method described in DIN EN ISO 10534-2. The normal acoustic impedance of an absorber configuration can be determined indirectly in the Kundt's tube by measuring sound pressure at different distances from the sample to separate the incident and reflected fraction of the sound wave and then calculating the acoustic impedance at the boundary surface. The results were averaged over three different samples of the same absorber type and the results for each sample were obtained by averaging four consecutive measurements. Taking into account the size of the loudspeaker and the tube diameter reasonable results can be expected from 200Hz to 8kHz.

Document downloaded by @DAEL, 2026-11-20 03:57:21 - personal use only

porous absorber is given by simple 1D transmission line equations:

$$Z(\Theta_i) = \frac{Z_a}{\cos\Theta_a} \coth\left(\Gamma_a \cos\Theta_a d\right), \tag{7}$$

where Θ_i is the incident angle and Θ_a is the complex refracted angle inside the porous absorber, which can be calculated from the law of refraction for lossy media:

$$\frac{\sin(\Theta_a)}{\sin(\Theta_i)} = \frac{\mathrm{j}k_0}{\Gamma_a}. \tag{8}$$

As was already mentioned, acoustic surface impedances can be assigned as Robin boundary conditions in fluid FEM simulations, but in a strict sense the angle of the incident sound wave needs to be a-priori known in order to assign the 'right' impedance to the simulation boundary. Since this is generally not the case, we often confine ourselves to using normal incidence impedances as boundary conditions. However, this simplification is only admissible if the absorber configuration can in good approximation be considered as 'locally reacting'. Following Mechel [10, pp. 39ff], we denote an absorber configuration 'locally reacting' if (a) the interaction between the incident sound and the absorber is fully described by the absorber characteristics at the specific location where we observe p and v_n and (b) sound propagation inside the absorber is only possible in the normal direction to the boundary surface. In this case the acoustic impedance is independent of the angle of incidence and thus the specification of the normal incidence impedance is valid irrespective of the actual angle of incidence. For a given absorber the assumption of 'local reaction' can be tested by considering the law of refraction for lossy media (cf. eq. (8)). The refracted angle is only close to zero for all Θ_i if $|\Gamma_a| >> k_0$, which is generally considered true for porous absorbers with high flow resistivity, due to the high damping term in the propagation constant Γ_a (cf. eq. (3)). On the other hand we denote materials with non-negligible wave propagation parallel to the boundary layer as 'laterally reacting'. In the case of porous absorbers such materials generally show increased damping as the angle of incidence rises. This is due to the fact that as the incident angle Θ_i and thus also Θ_a increase the actual path length of the sound wave travelling inside the porous absorber is extended and consequently the damping increases.

In order to alleviate the problem of the a-priori unknown angle of incidence, we can adapt an approach which is common practice in GA based simulations. Instead of using normal incidence boundary data in our simulations we can calculate boundary data for 'diffuse' or 'field' incidence[3]. The field incidence surface admittance can be obtained by averaging the surface admittance over all solid angles on a spherical cap with $0° < \Theta_i < 78°$. The corresponding field incidence impedance is then obtained by simple inversion of the admittance term:

$$A_{field} = \frac{\int_{0°}^{78°} A(\Theta_i)\sin(\Theta_i)\,\mathrm{d}\Theta_i}{\int_{0°}^{78°} \sin(\Theta_i)\,\mathrm{d}\Theta_i},$$

$$\text{and} \quad Z_{field} = \frac{1}{A_{field}}. \tag{9}$$

Averaging admittances instead of impedances appears admittedly quite arbitrary and it would of course also be possible to obtain a field incidence impedance by directly averaging the angle dependant impedances. Although we could unfortunately not find a good reason to favor the one or the other, we can at least state that both methods yield only marginally different results. More importantly, it has to be mentioned that in 2005 Takahashi [12] suggested a different formula for the calculation of the field incidence admittance, which introduces an additional cosine term in the integrals, like it is also found in the so-called Paris formula [13] for the diffuse field absorption coefficient[4] [14]. Again, we found that the differences between our formula and the formula presented by Takahashi turned out to be rather small. However, from a theoretical point of view we think that our formula without the cosine term in the integrals is more appropriate, since the cosine term in the formula for the diffuse field absorption coefficient does not stem from the averaging process but from the fact that we only integrate over the surface normal fractions of sound intensity $I_n = I\cos(\Theta_i)$, when we want to calculate the ratio of absorbed to incident sound power under diffuse incidence conditions.

Using field incidence impedances has the advantage that in the case of laterally reacting materials and field incidence the average damping of the porous absorber is not underestimated as would be the case with normal incidence impedances.

We can now use the definitions of Γ_a and Z_a of the Zwikker/Kosten and the Komatsu model presented in section 3.1 to calculate the acoustic impedance of a porous absorber for normal and field incidence conditions.

3.3. Coupled 3D-FE absorber model according to the Zwickker/Kosten theory

As was already mentioned the 3D-FE porous absorber model used in this study is based on the Zwikker/Kosten EHF model. Since the porous absorber is modelled as a damped fluid with only a pressure degree of freedom the finite element formulation is very similar to that of the fluid

[3] Since ideally diffuse conditions can generally not be obtained in typical rooms, the term 'field incidence' has emerged and is often referred to in building acoustics (see for example [11, p. 426f]). Field incidence assumes that angles of incidence are restricted to being equally probable between 0°-78°. Hopkins [11] states that the upper boundary for the angles of incidence is mostly empirically motivated and somehow lacks a physical meaning. However, the value of 78° has been adapted in many publications because of its commonly observed good fit with measured data.

[4] Takahashi simply replaces the angle dependent absorption coefficients in the formula for the diffuse field absorption coefficient by the corresponding admittances:

$$A^*_{field} = \frac{\int_{0°}^{78°} A(\Theta_i)\sin(\Theta_i)\cos(\Theta_i)\,\mathrm{d}\Theta_i}{\int_{0°}^{78°} \sin(\Theta_i)\cos(\Theta_i)\,\mathrm{d}\Theta_i}$$

Document downloaded by @DAEL, 2026-11-20 03:57:21 - personal use only

domain (see section 2). We can thus write a Helmholtz type equation for the porous absorber as follows:

$$\Delta p - \Gamma_a^2 p = 0 \quad \text{and} \quad v = \frac{1}{Z_a} \cdot p, \tag{10}$$

with the complex propagation constant and characteristic impedance taken from equations (3) and (4). The corresponding FE formulation for the porous absorber can be derived following the same steps as for the fluid model, where we use the same system matrices $\mathbf{K}_F$, $\mathbf{M}_F$ and $\mathbf{B}_F$:

$$\frac{\mathrm{j}\omega}{\left(\mathrm{j}\omega\frac{\chi}{\sigma_v} + \frac{\Xi}{\rho_0}\right)} \left(\mathbf{K}_F + (\mathrm{j}\omega\frac{\sigma_v \Xi}{\rho_0} - \omega^2\chi)\mathbf{M}_F\right)\mathbf{p} = \mathrm{j}\omega\mathbf{B}_F\,\mathbf{v_n}. \tag{11}$$

With regard to the boundary representation in acoustic FE simulations, it is important to point out the differences between a Robin boundary condition, based on an impedance calculated from the Zwikker/Kosten model for a specific angle of incidence and a coupled 3D-FE absorber model based on the same Zwikker/Kosten theory. It can be said, that the 3D absorber model adjusts the acoustic surface impedance to the right value depending on the actual angle of incidence in the simulation. Thus, in the case where the angle of incidence on a boundary layer is a-priori known and we assign the corresponding impedance to this boundary, we expect that both models yield the same results for the sound field in the room. In order to show that, we have run preliminary simulations in a tube model which was excited on one side and terminated by a porous absorber on the other side. The simulations were run for frequencies below the cut on frequency of the lowest lateral eigenmode of the tube so that only plane wave propagation was possible in the direction along the tube. The porous absorber was modelled (a) with its exact dimensions using the 3D-FE absorber model and (b) by an impedance boundary condition which was calculated for normal incidence. As expected the results of the simulations showed a perfect match, which confirms that the underlying theory for the 3D absorber model and the calculation of the impedance boundary condition are the same.

4. Comparison of different boundary representations on the sound field in a damped scale model room

4.1. Room geometry

In order to compare the influence of different boundary specifications on the sound field in a room, measurements and FE simulations have been conducted in a scale model room with a well defined geometry and variable boundary conditions. The rectangular room is made of 38 mm thick MDF (medium density fibreboard) plates and measures 1.25 × 1.00 × 0.75 m^3. Three walls of the room are planked with MDF wedges that are chamfered at different angles from 5° to 9° in order to avoid flutter echoes in

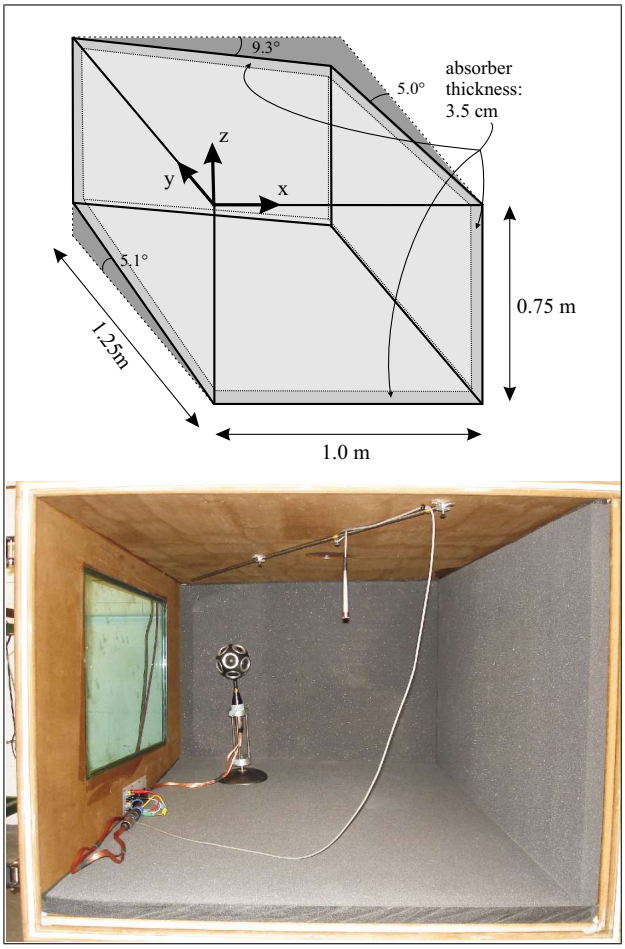


Figure 1. Drawing and photo of scale model room with absorption applied to three walls.

the room. Measurements and simulations have been conducted for three different source receiver configurations. Simulation results are reported for the frequency range from 100 Hz to 1.4 kHz in 2 Hz steps. Figure 1 shows the scale model room with the small dodecahedron source, the measurement microphone and pu foam applied to three walls in the room.

In the FE simulations we approximate the dodecahedron source by a point source and assign a real impedance to the MDF walls, which we estimate from reverberation time measurements in the empty room. In order to get conforming levels for simulation and measurement we normalize the measured and simulated pressure results to the sound pressure in 1 m distance in the free-field, where we use the formula for an ideal point source to normalize the simulations and we use anechoic measurements of the small dodecahedron to normalize the measurements. Throughout the simulations we keep all parameters constant except for the boundary specification of the porous absorber. A comparison of measurements and FE simulations in the same scale model environment without porous absorbing material, which is presented in [15], had shown that an excellent match between measured and simulated frequency responses and absolute sound levels can be achieved with this dodecahedron loudspeaker and the applied normaliza-

Document downloaded by @DAEL, 2026-11-20 03:57:21 - personal use only

tion technique. We are thus confident that the observed differences between measurement and simulation in the damped scale model room, which we will discuss in the following section, are predominantly caused by the representation of the porous absorber materials at the room boundaries.

4.2. Materials

For our simulations we use two different rigidly backed porous materials with largely different flow resistivities in order to emphasize the differences between locally and laterally reflecting materials. The first material is a typical porous PU foam, with thickness $d = 35$ mm, and measured parameters $\Xi = 5.4$ kPa s/m^2 and $\sigma_v \approx 0.97$. The second material is a Rockwool mineral wool of the same thickness with measured parameters $\Xi = 45$ kPa s/m^2 and $\sigma_v \approx 0.97$. In addition to the measured absorber parameters we use reasonable estimated values $\chi = 1$ and $\kappa_{eff} = 1.2$ for both materials[5].

Figure 2 shows a comparison of the measured (Kundt's Tube) and calculated (Zwikker/Kosten and Komatsu) absorption coefficients for normal incidence for both materials. Although we use complex impedances as boundary conditions in our FE models we plot absorption coefficients to facilitate interpretation of the results. For the PU foam the Komatsu model gives a good match with the measured absorption coefficients, whereas the Zwikker/Kosten model yields on average about 0.15 less absorption. For the Rockwool mineral wool both models show a reasonable match with the measured data.

Figures 3 and 4 show a contour plot of the absorption coefficient and a comparison of normal incidence and field incidence impedance curves for both materials. These curves were calculated using the Komatsu model which showed on average the best match with the measured data from the Kundt's Tube[6]. As expected, it can be seen that the PU foam with low flow resistivity shows a much stronger angular dependency of the absorption coefficient than the mineral wool with high flow resistivity. However, it is important to mention that only looking at absorption curves can be somehow misleading in this context, since the absorption coefficient always shows an angular dependency due to the change in the characteristic impedance of air $Z_0' = Z_0/cos(\Theta_i)$ even for perfectly locally reacting materials. Consequently, an angular dependence of the absorption coefficient does by itself not necessarily indicate an angular dependence of Z and thus a 'non-locally reacting' material. However, looking at the results from Figure 4 indicates that in the case of the pu foam the angular dependence of α is strongly driven by the angular dependence of Z whereas in the case of the Rockwool absorber the slight changes in α are mostly caused by the change in Z_0'. In section 4 we will discuss how the non-locally reflecting characteristics of the pu foam affect the simulation results when an impedance boundary condition is used and we will investigate if improved results can be obtained with the 3D absorber model, which fully captures the angular dependency of the acoustic impedance of the absorber.

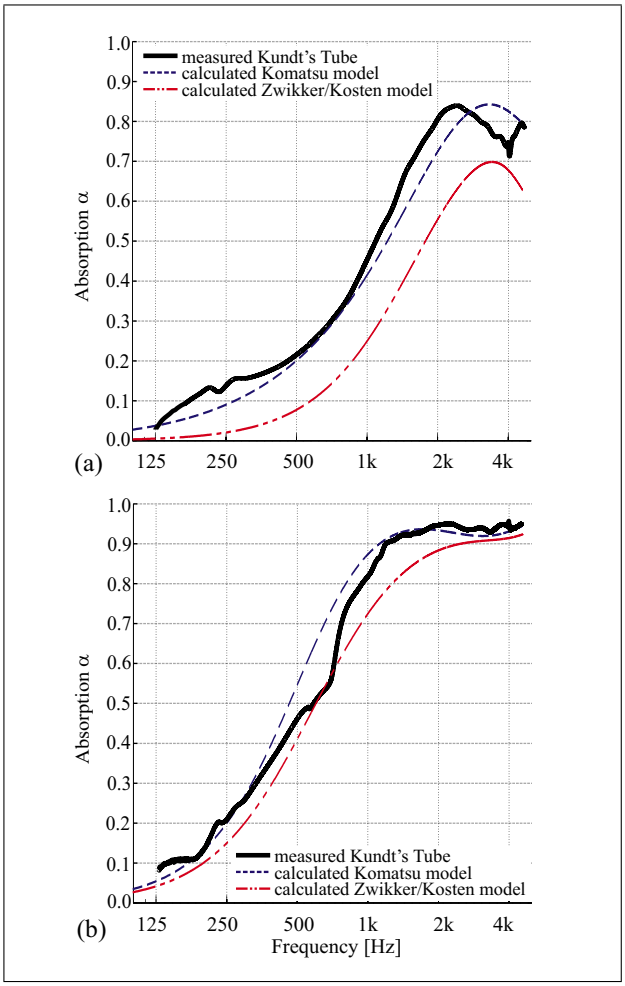


Figure 2. Absorption of (a) 35 mm PU foam (flow resistivity 5.4 kPa s m^2) and (b) 35 mm Rockwool mineral wool (flow resistivity 45 kPa s m^2) for normal incidence calculated from measured and modelled impedances.

4.3. Results and discussion

We first want to discuss the effect of angular dependence of the acoustic impedance on the simulated sound field in our model room. We have therefore run FE simulations where we consider the acoustic characteristics of the absorbing room boundaries by (a) an acoustic impedance calculated for normal incidence and (b) a 3D-FE absorber model, both of which are derived on the basis of the Zwikker/Kosten EHF model. The simulations were run for the PU foam and the Rockwool mineral wool. Additionally, as a reference, we have carried out measurements in

[5] Although from a theoretical point of view a value of $\kappa_{eff} = 1.41$ would have been be more suitable, since we are dealing with rather low frequencies in the FE simulations, the value was adjusted to 1.2 for better agreement with the measured absorption data. However, it has to mentioned that the influence of different values of κ_{eff} on the absorption data is rather small.

[6] The respective curves calculated with the Zwikker/Kosten model yield qualitatively the same results and are therefore not reported here.

Document downloaded by @DAEL, 2026-11-20 03:57:21 - personal use only

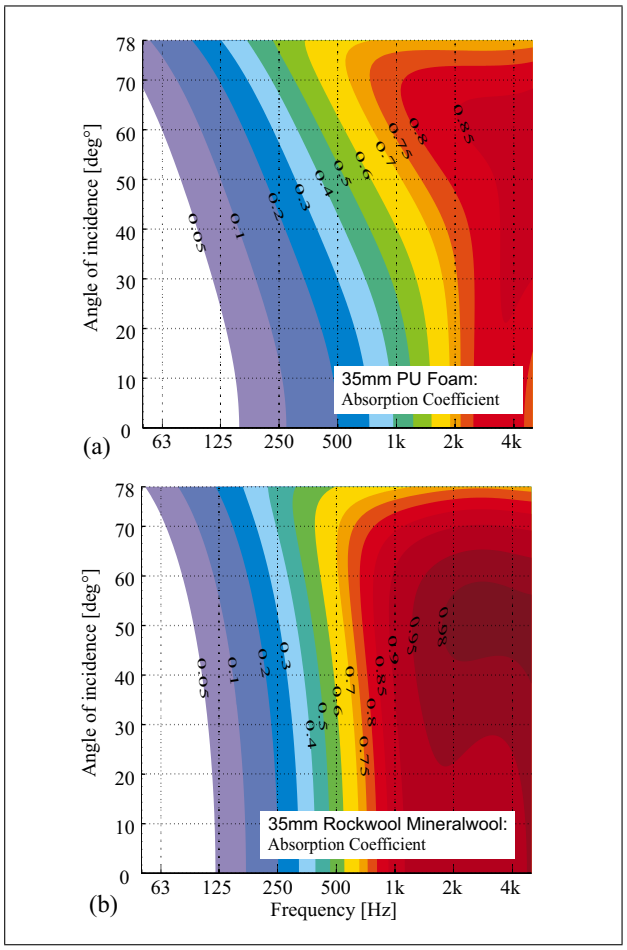


Figure 3. Contour Plot of the absorption coefficient of PU foam and Rockwool mineral wool for different angles of incidence calculated from the Komatsu model.

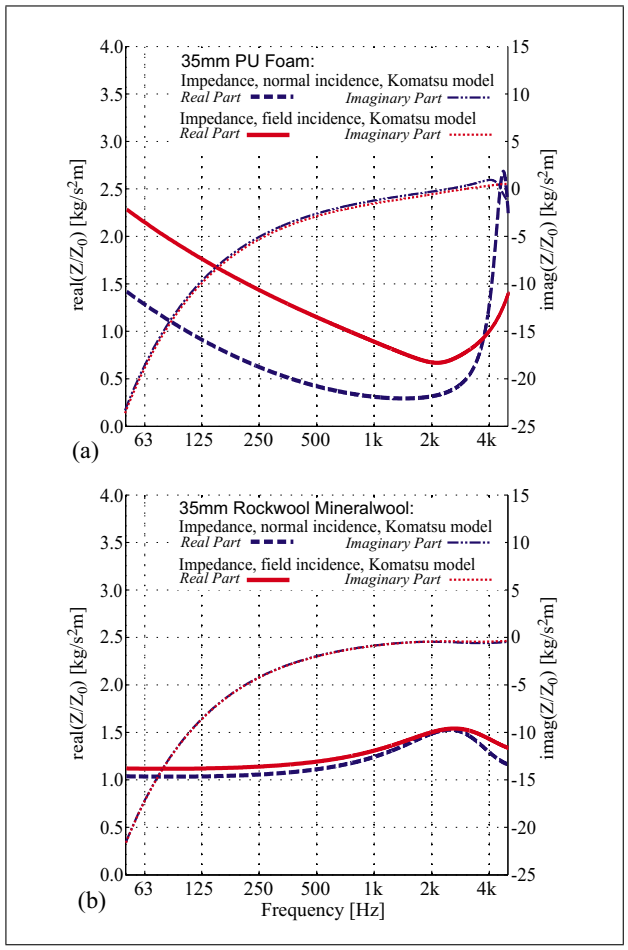


Figure 4. Comparison of normal incidence and field incidence acoustic surface impedance for PU foam and Rockwool mineral wool calculated from the Komatsu model.

the scale room where three walls were covered with the PU foam (see Figure 1) and the Rockwool mineral wool respectively. Since the two different boundary representations are all based on exactly the same absorber model, it is interesting to ask the question in which cases we expect different results. Figure 5 shows the logarithmic amplitude and the group delay [7] of the resulting normalized RTFs. It can be seen that for the mineral wool the two boundary representations yield almost identical results which show a reasonably good match with the measured curve. This is due to the fact that the mineral wool shows almost no angular dependence of the acoustic impedance in the considered frequency range (see Figure 4). In other words this means, that due to its high flow resistivity the mineral wool absorber can be classified as almost perfectly 'locally reacting'. Since all incident waves are refracted to the normal direction inside the porous absorber there is no benefit from the 3D FE absorber model, since the 1D transmission line model (used to calculate the acoustic impedance for normal incidence) fully captures the acoustic behaviour of this absorber.

In the case of the PU foam things look different. Due to the non-negligible angular dependence of the acoustic characteristics of the pu foam, the results obtained with the impedance for normal incidence show considerably higher quality factors and thus lower damping of the room eigenmodes than is obtained with the 3D FE absorber model. Compared to the measurements in the model room we find that the 3D absorber model yields very good results, whereas the normal incidence impedance strongly underestimates the damping in the room. Thus, we conclude that in the case of 'non-locally reacting' absorbers, a normal incidence acoustic impedance does generally underestimate the absorption characteristics of a room boundary, as was expected from our explanations in section 3.2.

In the next step we want to investigate the performance of the field incidence impedance model. Figure 6 shows the results of these simulations, where we use the Zwikker/Kosten model and the Komatsu model to calculate the field impedances of the pu foam and mineral wool respectively. For the pu foam, it can be seen that the RTFs calculated with the field incidence impedances as bound-

[7] The group delay τ_g is given in seconds and is defined as the rate of change of the total phase shift ϕ with respect to the angular frequency ω: $\tau_g = -\mathrm{d}\phi/\mathrm{d}\omega$. We prefer plotting group delay over plotting the unwrapped phase because of the smaller range of values in the group delay plot.

Document downloaded by @DAEL, 2026-11-20 03:57:21 - personal use only

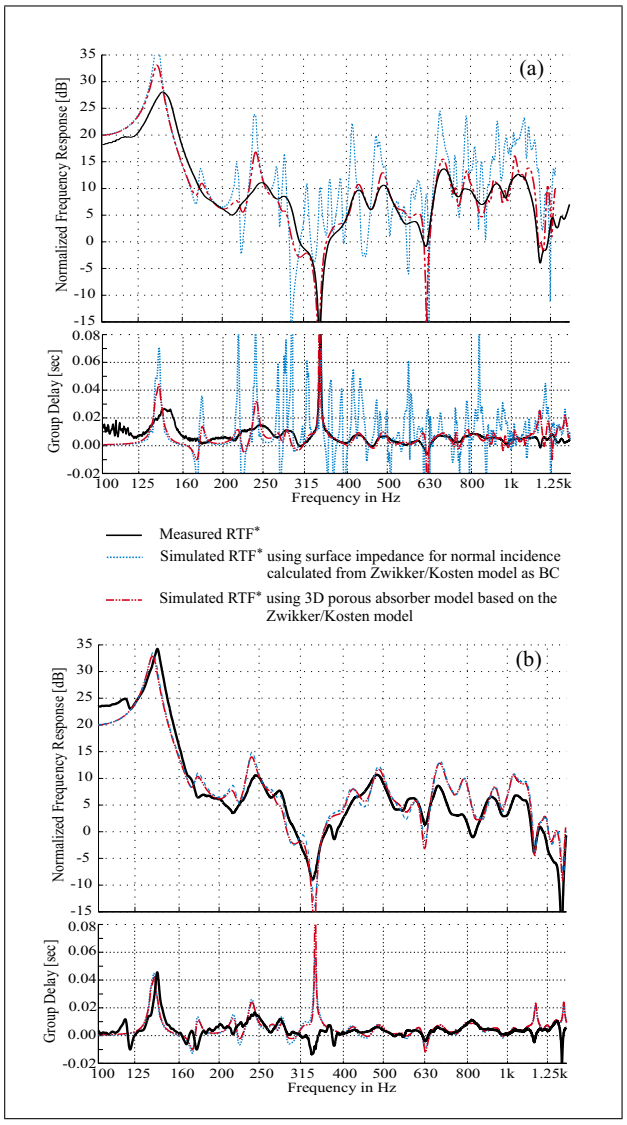


Figure 5. Measured and simulated room transfer functions (RTF) using different boundary models for porous absorber. (*) Measured and simulated room transfer functions are normalized to sound pressure in 1 m distance in the free field with the respective source. (a) Room with 35 mm PU foam on 3 walls, (b) Room with 35 mm Rockwool on 3 walls.

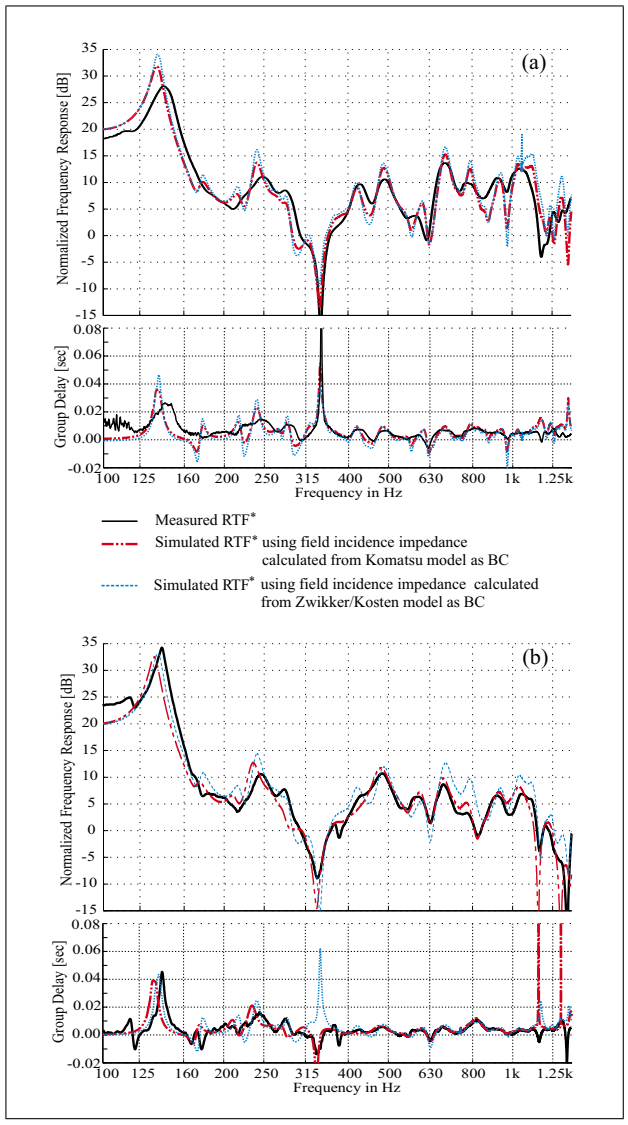


Figure 6. Measured and simulated room transfer functions (RTF) using different boundary models for the porous absorber. (*) Measured and simulated room transfer functions are normalized to sound pressure in 1 m distance in the free field with the respective source. (a) Room with 35 mm PU foam on 3 walls, (b) Room with 35 mm Rockwool on 3 walls.

ary conditions yield a very good match with the measured RTF. However, although the absorption curves of the pu foam in Figure 2 show that the Komatsu model yields a better match with the measured data than is obtained from the Zwikker/Kosten model, only a slight improvement in the match of measured and simulated RTFs can be found by using the Komatsu model for the calculation of the field incidence impedances. It is also noteworthy that for the pu foam the field incidence impedance model yields comparably good results for the RTF as those obtained with the full 3D absorber model.

In the case of the mineral wool we find that using the field incidence impedance calculated from the Komatsu model yields a slightly better match with the measured RTF (especially in the range from 600 Hz–1 kHz) than the respective impedance calculated from the Zwikker/Kosten model, which gives almost identical results to those obtained from the normal incidence impedance or the 3D FE absorber model based on this model. Only at around 345 Hz, we observe a significant difference between both simulations in the group delay. Taking into account that we find two very close eigenfrequencies of the rigid room in this frequency range[8] and further considering the sharp notch in the magnitude of the RTFs at about 345 Hz, it is believed that this difference is due to a strong resonant

[8] Due to limitations of the used FE solver, the eigenmodes could only be calculated for the empty room with rigid boundaries. In this case, eigenfrequencies were found at 344 Hz and 351 Hz. Due to the reduced speed of sound inside the porous absorber (compared to the propagation in air) the actual eigenfrequencies of the damped room are believed to be slightly lower.

Document downloaded by @DAEL, 2026-11-20 03:57:21 - personal use only

effect caused by a slight discrepancy in the room eigenmodes simulated with the different absorber models on the boundaries. Thus, even in the case of perfectly 'locally reacting' materials, where a simple normal incidence impedance suffices, the simulation results obviously depend on the applied absorber model and the corresponding impedance. The uncertainty in the RTF which is obtained by using different porous absorber models appears to be in a range of on average 1 to 2 dB.

5. Conclusions

The presented study investigates the influence of different boundary representations of a porous absorber on the simulated sound field in small rooms. In particular we use an 'equivalent homogeneous fluid' (EHF) based 3D FE absorber model as well as acoustic surface impedances for normal and field incidence conditions to model the acoustic characteristics of homogeneous porous absorbers in room acoustic FE simulations. We a-priori distinguish porous absorbers into 'laterally' and 'locally' reacting absorbers, which indicates if the acoustic surface impedance Z depends on the angle of the incident sound wave. Furthermore we show that the assumption of local reaction can be tested by the law of refraction for lossy media, where the propagation constant of the porous absorber can be estimated using an appropriate EHF model.

In our simulations we use a light porous pu foam with strong angular dependence of Z and a heavy mineral wool with almost no angular dependence of Z. As is expected the results of the study confirm that using normal incidence acoustic impedances as boundary conditions in room acoustic FE simulations is only valid, if the considered absorber is in good approximation 'locally reacting'. Moreover the results show that in the case of 'laterally' reacting absorbers a normal incidence impedance generally leads to a considerable underestimation of the damping in a room, while the 3D FE absorber model and the field incidence impedance show considerably improved simulation results, since these models capture the increased damping that is obtained for angular incidence. Interestingly, although the field incidence impedance does only account for the angle of incidence on an average basis, the simulations with field incidence impedances show comparably good results to those obtained with the 3D FE absorber model. Taking into account the higher computational cost and model complexity associated with a 3D FE absorber model, we conclude that a field incidence impedance adequately captures the characteristics of both 'locally' and 'laterally' reacting porous absorbers in room acoustic FE simulations and that it is possible to obtain an excellent agreement between measured and simulated results with this approach. However, it has to be mentioned that the simulation results obviously depend on the underlying porous absorber model and the quality of its input data.

Acknowledgement

The authors would like to thank A. Franck, who mainly developed the utilized FE-solver *SoundSolve* while working as a research assistant at ITA of RWTH Aachen University.

References

[1] M. Vorländer: Auralization. Springer-Verlag, Berlin, 2007.

[2] F. Ihlenburg: Finite element analysis of acoustic scattering. Applied Mathematical Sciences, vol. 132. Springer-Verlag, New York, 1998.

[3] C. Zwikker, C. Kosten: Sound Absorbing Materials. Elsevier, Amsterdam, 1949.

[4] J. W. Strutt, Lord Rayleigh: Theory of sound (two volumes). New York, Dover Publications, 1877; 2nd Ed. 1945 re-issue.

[5] J. Allard, N. Atalla: Propagation of sound in porous media: Modeling sound absorbing materials. 2nd edition ed. John Wiley and Sons, 2009.

[6] M. Delany, E. Bazley: Acoustical properties of fibrous absorbent materials. J. Applied Acoust. **3** (1970) 105–116.

[7] T. Komatsu: Improvement of the Delany-Bazley and Miki models for fibrous sound-absorbing materials. Acoustic Science & Technology **29** (2008) 121–129.

[8] M. A. Biot: Theory of propagation of elastic waves in a fluid-saturated porous solid. I. Low-frequency range. J. Acoust. Soc. Am. **28** (1956) 168–178.

[9] F. Mechel: Schallabsorber Bd. 2. Innere Schallfelder – Strukturen. S. Hirzel Verlag, Stuttgart, 1995.

[10] F. Mechel: Schallabsorber Bd. 1. Äußere Schallfelder – Wechselwirkungen. S. Hirzel Verlag, Stuttgart, 1989.

[11] C. Hopkins: Sound Insulation. Butterworth-Heinemann, 2007.

[12] Y. Takahashi, T. Otsuru, R. Tomiku: In situ measurements of surface impedance and absorption coefficients of porous materials using two microphones and ambient noise. J. Applied Acoust. **66** (2005) 845–865.

[13] E. Paris: On the reflexion of sound from a porous surface. Proc. R. Soc. Lond. **115** (1927) 407–419.

[14] H. Kuttruff: Room Acoustics. Taylor & Francis, 4th edition, 2000.

[15] M. Aretz: Specification of realistic boundary conditions for the FE simulation of low frequency sound fields in recording studios. Acta Acustica United with Acustica **95** (2009) 874–882.

Document downloaded by @DAEL, 2026-11-20 03:57:21 - personal use only